Identification and functional expression of the *Arabidopsis thaliana* vacuolar glucose transporter 1 and its role in seed germination and flowering

Sirisha Aluri and Michael Büttner*

*Molekulare Pflanzenphysiologie, Universität Erlangen–Nürnberg, Staudtstrasse 5, D-91058 Erlangen, Germany

Edited by Maarten J. Chrispeels, University of California at San Diego, La Jolla, CA, and approved December 18, 2006 (received for review November 20, 2006)

Sugar compartmentation into vacuoles of higher plants is a very important physiological process, providing extra space for transient and long-term sugar storage and contributing to the osmoregulation of cell turgor and shape. Despite the long-standing knowledge of this subcellular sugar partitioning, the proteins responsible for these transport steps have remained unknown. We have identified a gene family in *Arabidopsis* consisting of three members homologous to known sugar transporters. One member of this family, *Arabidopsis thaliana* vacuolar glucose transporter 1 (*AtVGT1*), was localized to the vacuolar membrane. Moreover, we provide evidence for transport activity of a tonoplast sugar transporter based on its functional expression in bakers' yeast and uptake studies in isolated yeast vacuoles. Analyses of *Atvgt1* mutant lines indicate an important function of this vacuolar glucose transporter during developmental processes like seed germination and flowering.

glucose transport | vacuole | tonoplast

Sugars play important roles as nutrients as well as signal molecules during the life cycle of higher plants. The distribution of sugars within plants requires several essential transport steps across membranes on the subcellular level but they also are used for long-distance transport (1–3). The latter is required when the green phototrophic parts of the plant supply nonphotosynthetic tissues and organs with assimilates, mainly in the form of sucrose (4, 5). Sucrose is then either directly transported into sink cells or, after cleavage by an extracellular invertase, is taken up in the form of the hexoses glucose and fructose (6). On the other hand, sugars can also be distributed on the single-cell level into different organelles, depending on their actual requirements. During the day, many plant species use up to half of their assimilated carbon for starch synthesis and transient storage in the chloroplast (7). In addition, sugars can be imported into the vacuoles for transient or long-term storage. Because some agriculturally important plants like sugar beet (8–11) and sugar cane (12) store a considerable amount of sugars in the vacuoles of storage organs, there is a longstanding interest in this specific type of sugar partitioning.

Experiments on isolated vacuoles have provided biochemical evidence for the uptake of both sucrose and hexoses into these organelles (12–14). Interestingly, both passive diffusion and active transport have been suggested as the uptake mechanism for these sugars (15–17). The transport of sugars across membrane barriers is greatly mediated by transport proteins, which catalyze either passive (but selective) diffusion or energy-dependent active transport, thereby allowing accumulation of sugar substrates. Although the transport proteins for the uptake of sugars across the plasma membrane and into the cell for sucrose (1, 3, 5) and for hexoses (3, 18, 19) have been identified and greatly characterized for a variety of plants, very little is known about the corresponding transporters in the tonoplast. The vacuolar localization of a putative hexose transporter homolog has been suggested in sugar beet as the result of in vitro colocalization studies (20), but so far the evidence for transport activity has not been provided and further *in vivo* localization studies are required to prove that such a protein is indeed a vacuolar sugar transporter. Recently, a proteomics approach and transient expression studies using GFP fusion proteins have indicated that a sucrose transporter from barley, *HvSUT2*, could localize to the tonoplast (21). However, results from expression studies of *HvSUT2* in bakers' yeast (22) as well as immunolocalization to the plasma membrane of its closest homologs in tomato (LeSUT4) and potato (StSUT4) plants are contrary to this finding (23).

Measurements of sugar concentrations made by using a nonaqueous fractionation technique in a variety of plants revealed that in leaves the vast majority of glucose is found in the vacuole, but sucrose seems to be found mainly in the cytoplasm (24–27). Even if the vacuole can account for >90% of the total volume in leaf mesophyll cells, the concentration of glucose in the vacuole is still higher than in the cytoplasm. Thus, an active import of glucose into the vacuole has to be postulated to allow this accumulation.

We have investigated previously uncharacterized genes within the major facilitator superfamily (28) that show homology to known hexose transporter genes in *Arabidopsis* (*AtSTPs*). Here we demonstrate that one of these *AtSTP* homologs, *Arabidopsis thaliana* vacuolar glucose transporter 1 (*AtVGT1*), is a hexose transporter of the vacuolar membrane and as such has a significant impact on different aspects of plant development.

Results

Identification of a Sugar Transporter Family in *Arabidopsis*. Our *in silico* analyses revealed a high degree of sequence homology to the known *AtSTP* gene family of monosaccharide transporters in *Arabidopsis* for three previously unknown ORFs: At3g03090, At5g17010, and At5g59250. We generated the corresponding cDNAs comprising the entire ORFs by RT-PCR from flowers in the case of At3g03090 and whole-plant mRNA in the cases of At5g17010 and At5g59250. Sequence determination confirmed the predicted exon/intron structure for all three genes with 13 introns at conserved positions and characterized them as a distinct gene family within the *Arabidopsis* monosaccharide transporter-like superfamily (www.arabidopsis.org/info/genefamily/genefamily.html). At3g03090 and At5g17010 show the highest degree of protein sequence conservation (71% similarity and 62% identity), whereas At5g59250, the most distant member of this family, shares only 60% (46%) and 49%

Author contributions: M.B. designed research; S.A. performed research; S.A. and M.B. analyzed data; and M.B. wrote the paper.

The authors declare no conflict of interest.

This article is a PNAS direct submission.

Abbreviation: AtVGT1, *Arabidopsis thaliana* vacuolar glucose transporter 1.

*To whom correspondence should be addressed. E-mail: mbuettne@biologie.uni-erlangen.de.

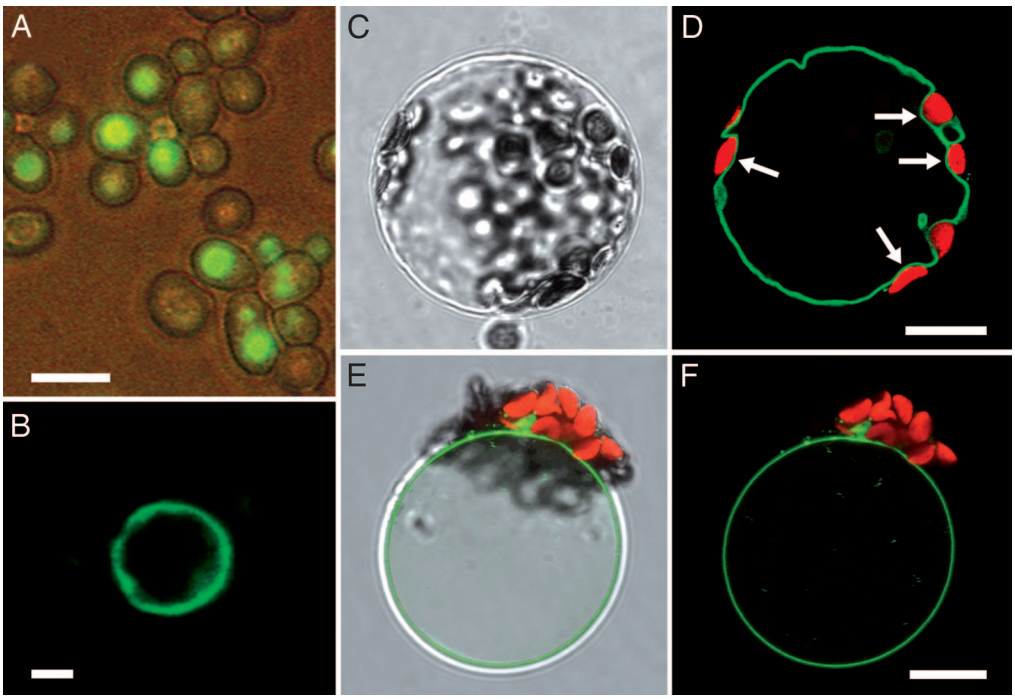

Fig. 1. Tonoplast localization of the AtVGT1–GFP fusion protein in yeast and *Arabidopsis*. (*A* and *B*) In yeast, the AtVGT1–GFP fusion protein is localized in internal membranes (*A*) and after separation of subcellular compartments can only be seen in vacuolar membranes (*B*). (Scale bars, *A*, 5 μm; *B*, 1 μm.) (*C* and *D*) When expressed transiently in *Arabidopsis* protoplasts, the AtVGT1–GFP fusion protein is clearly inserted into the tonoplast, which separates the vacuolar volume from the cytoplasm containing chloroplasts (white arrows). (*E* and *F*) After protoplast lysis, GFP fluorescence can only be seen in the remaining membrane of intact vacuoles. (Scale bar, 10 μm.)

(36%) similar (identical) amino acids with At3g03090 and At5g17010, respectively. Hydropathy analyses of the protein sequences predict 12 transmembrane helices for the newly identified hexose transporter homologs. In the current study, we focus on the characterization of one of the *Arabidopsis* genes, At3g03090 (*AtVGT1*).

Heterologous Expression in *Saccharomyces cerevisiae* Reveals Vacuolar Localization of AtVGT1. Because of its homology to known monosaccharide transporters, *AtVGT1* was tested for the ability to complement a hexose-transport-deficient yeast mutant EBY.VW4000 (29). Whereas the expression of some of the known *Arabidopsis* hexose transporters could restore growth of this yeast mutant on glucose (30, 31), expression of At3g03090 did not complement the hexose-transport-deficient null mutant (data not shown). Therefore, to verify expression and to determine a possible subcellular localization, a *GFP*-tagged version of the *AtVGT1* gene was expressed in this yeast strain. As shown in Fig. 1, GFP fluorescence was not seen in the plasma membrane but rather in internal structures strongly resembling vacuoles (Fig. 1*A*). When we then isolated vacuoles from the *AtVGT1*/*GFP*-expressing yeast strain, the fusion protein was clearly confined to the vacuolar membrane, as shown by the GFP fluorescence (Fig. 1*B*).

AtVGT1 Also Localizes to the Tonoplast *in Planta*. The tonoplast localization of the GFP fusion protein observed in transgenic yeast lead us to investigate the subcellular localization of the At3g03090 gene product in *Arabidopsis*. To this end, we transiently expressed a *GFP* fusion in *Arabidopsis* protoplasts. Confocal microscopy allowed a clear assignment of the fusion protein to the tonoplast (Fig. 1 *C* and *D*), most obvious in the regions where chloroplasts are seen (Fig. 1*D*, white arrows). Moreover, after protoplast lysis by mild osmotic shock, GFP fluorescence was seen only in the membrane of the remaining intact vacuoles (Fig. 1 *E* and *F*), reconfirming the vacuolar localization of AtVGT1 *in planta*.

AtVGT1 Mediates Active Sugar Transport into Yeast Vacuoles. To investigate the transport properties of AtVGT1, we again used bakers yeast as a heterologous expression system and isolated vacuoles for transport assays. To first test the functionality of the isolated vacuoles, we verified uptake competence for amino acids as described by Ohsumi and Anraku (32). ATP-dependent [^{14}C]lysine uptake demonstrated proper function of the vacuolar ATPase (data not shown). These vacuoles were then further tested for glucose-uptake activity. Whereas no glucose-uptake was detected in the control strain expressing *AtVGT1* in antisense (SAY114as), vacuoles of the *AtVGT1*-expressing strain SAY114s showed a time-dependent accumulation of ^{14}C-labeled glucose (Fig. 2*A*). Furthermore, omitting ATP in the reaction-mix completely abolished glucose uptake, strongly suggesting the presence of an energy-dependent transport mechanism that would allow accumulation of the substrate against a concentration gradient. We further tested other hexoses and sugar alcohols, which are known to accumulate in vacuoles under certain conditions, and the pentose xylose. As seen in Fig. 2*B*, none of the other sugars was taken up by SAY114s vacuoles except fructose, which is also transported but only to 42% of the glucose transport rate. Fructose is a sugar also found in plant vacuoles in appreciable concentrations. Finally, concentration-dependent rates for AtVGT1-mediated glucose uptake were determined, and a K_m of 3.7 mM was calculated from the Lineweaver–Burk plot (Fig. 2*B Inset*). Because of the demonstrated vacuolar localization and the described transport properties, we named the transporter AtVGT1.

***AtVGT1* Is Expressed in All Above-Ground Plant Tissues.** To investigate the expression profile of the vacuolar glucose transporter

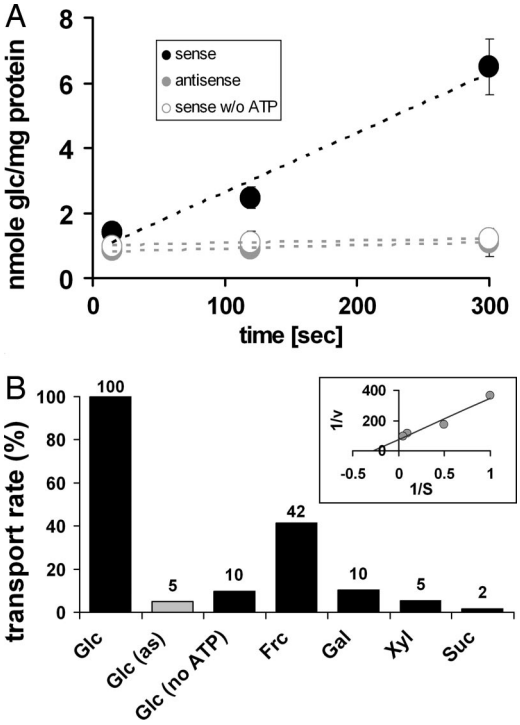

Fig. 2. Transport properties of AtVGT1 in yeast. (*A*) The transport capacity for glucose of yeast cells expressing the *AtVGT1* cDNA in sense orientation (strain SAY114s; black circles) or antisense orientation (strain SAY114as; gray circles) in the presence of ATP and in sense orientation in the absence of ATP (white circles) was analyzed. Values represent the mean of seven independent transport analyses for sense and antisense and three for sense without added ATP (±SE). (*B*) Substrate specificity for AtVGT1 is shown as relative uptake rates of different sugars in *AtVGT1*-expressing yeast cells (sense: black bars; antisense: gray bar), determined at an initial outside concentration of 1 mM and in the presence of 4 mM ATP if not stated otherwise. (*Inset*) Lineweaver–Burk plot of concentration-dependent glucose uptake. v, nmol·sec^{-1}; S, mM. All data represent average values of at least two independent transport tests.

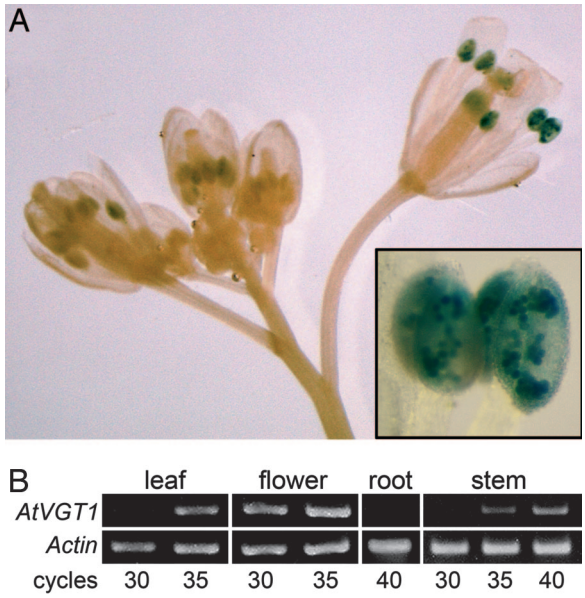

Fig. 3. *AtVGT1* expression analyzed by *GUS* reporter plants and RT-PCR. (*A*) Influorescence with GUS histochemical staining showing reporter expression in anthers of GUS reporter plants starting from flower stage 10, according to Bowman (53). (*Inset*) Anthers at higher magnification showing GUS staining in pollen grains. (Magnification: ×10; *Inset*, ×66.) (*B*) RT-PCR analysis using equal amounts of total RNA from wild-type leaves, flowers, roots, and stems. PCRs with 30, 35, and 40 cycles were done with *AtVGT1*- or *Actin2*-specific primers.

gene that we identified, we generated transgenic reporter plants expressing the β-glucuronidase (GUS) gene under the control of the *AtVGT1* promoter. Analysis of the reporter plants revealed *AtVGT1* promoter activity only in anthers, where it was restricted to pollen grains (Fig. 3*A Inset*). RT-PCR experiments reconfirmed the gene's high rate of expression in flowers. However, using this method we also were able to detect the *AtVGT1* transcript in leaves and stems with lower but significant abundance, except in roots (Fig. 3*B*). To obtain an estimate of the relative *AtVGT1* expression levels in other tissues, the Genevestigator *Ar. thaliana* Microarray Database and Analysis Toolbox (ETH, Zurich, Switzerland) (33) was queried. According to this database, *AtVGT1* mRNA accumulates to significant levels in all developmental stages and all organs, except in roots. Higher *AtVGT1* transcript levels are found in the shoot apex and in seeds. We conclude that *AtVGT1* is expressed at low levels in all above-ground tissues and particularly strongly in pollen.

Analysis of Mutant Lines Carrying a T-DNA Insertion in the *AtVGT1* Gene Demonstrate a Role in Seed Germination and Flowering To assess the physiological importance of AtVGT1 transport function, we analyzed T-DNA insertion mutants obtained from the European *Arabidopsis* Stock Center (Fig. 4*A*). For two lines, SALK_000988 (insertion at position −1, 5′UTR) and SAIL_669_D03 (insertion at position +2762, intron 9), homozygousity of the T-DNA insertion and absence of *AtVGT1* transcript were verified by PCR analyses (Fig. 4 *B* and *C*). In the SALK_000988 line, the T-DNA insertion was detected by a specific PCR product (Fig. 4*B*, lane 3), but in contrast to the wild-type control (Fig. 4*B*, lane 2) no PCR product was obtained through the use of primers spanning the insertion site because of the size of the T-DNA (Fig. 4*B*, lane 4). The lack of *AtVGT1* transcript in the SAIL_669_D03 line was demonstrated by RT-

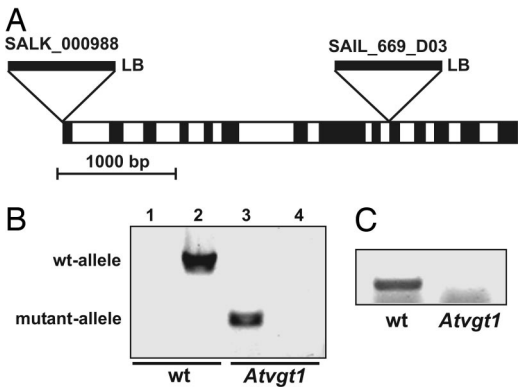

Fig. 4. Identification of T-DNA insertions in the *AtVGT1* gene. (*A*) The position and orientation of the T-DNA insertion in the *AtVGT1* gene of the mutant lines SALK_000988 and SAIL_669_D03. The gene has 13 introns (white boxes), and the insertions are located at position −1 (SALK line) and +2760 relative to the start codon. The orientation of the left border (LB) is indicated, and the opposite end of the insertion has not been characterized. (*B*) Genomic PCR analysis demonstrating homozygous T-DNA insertion in the SALK_000988 line. By using a T-DNA primer and a gene-specific primer, a 428-bp PCR product was amplified from mutant DNA (lane 3) but not from wild-type (wt) DNA (lane 1); whereas, by using gene-specific primers spanning the insertion site, a 1,788-bp PCR product was amplified from wild-type DNA (lane 2) but not from mutant DNA (lane 4). (*C*) RT-PCR analysis demonstrating the lack of *AtVGT1* transcript in the SAIL_669_D03 line. By using gene-specific primers spanning the insertion site, a 407-bp RT-PCR product was amplified from wild-type flower cDNA but not from mutant flower cDNA.

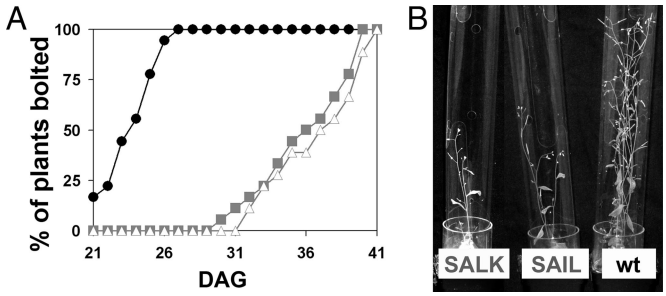

Fig. 5. Delay in flowering of *Atvgt1* mutant lines. (*A*) Initiation of flowering diagrammed as the percentage of plants showing growth of primary shoots was determined for Col-0 wild-type (wt) plants (black circles), SALK_000988 plants (gray squares), and SAIL_669_D03 plants (white triangles). (*B*) A*tvgt1* mutant lines in comparison with wild-type plants (Col-0) 1 week after the induction of flowering (36 days after germination).

PCR (Fig. 4*C*). Because *AtVGT1* is strongly expressed in flowers and shows above-average expression levels in the shoot apex, we particularly examined a possible influence of the *Atvgt1* knockout on flowering. As shown in Fig. 5, eliminating AtVGT1 transport function leads to a drastic delay in flowering. Under long-day conditions, wild-type plants started to grow primary shoots 21–26 days after germination. In contrast, under identical conditions *Atvgt1* mutant lines did not start bolting until 30–40 days after germination (Fig. 5*A*). However, this drastic delay in bolting did not lead to a complete absence of flowering because all *Atvgt1* mutant plants eventually produced shoots with flowers and seeds comparable with those produced by wild-type. In addition to this delayed flowering phenotype, we found that ≈20% of the *Atvgt1* mutant seeds did not germinate, indicating a function for *AtVGT1* also during processes like seed development and/or germination. The observed mutant phenotypes support a model in which vacuolar sugar accumulation is required for osmotic adjustment and turgor increase during developmental processes like seed germination and flowering.

Discussion

Despite longstanding knowledge of sugar transport across the tonoplast in higher plants, no vacuolar sugar transport protein could be isolated and characterized. We have identified a gene family in *Arabidopsis* consisting of three members with strong homology to known monosaccharide transporters. Besides the high sequence homology found within this family, the genomic gene structure is highly conserved with respect to position and number of introns. Although an average *Arabidopsis* gene carries five introns (34), 13 introns were found in all three genes of this family. A possible regulatory function of this feature can only be assumed, but it clearly distinguishes this family from other gene families within the major facilitator superfamily (28).

For one of these genes, *AtVGT1*, we demonstrated localization in *Arabidopsis* vacuoles by transient expression of a *GFP* fusion (Fig. 1). To analyze its transport properties, we expressed *AtVGT1* in bakers yeast. Because the corresponding transport protein is localized to the vacuolar membrane in yeast, we had to optimize a purification method to isolate transport-competent vacuoles from these yeast strains. Using this approach, we were able to demonstrate transport activity for the vacuolar sugar transporter AtVGT1. Further characterization revealed that AtVGT1 transports preferentially glucose with a K_M of 3.7 mM. To a much smaller degree, fructose (hexose) also was accepted, but no incorporation was obtained for sucrose (disaccharide) or mannitol (sugar alcohol). We also tested xylose (pentose) as a possible substrate because in several databases *AtVGT1* (At3g03090) is annotated as a putative sugar transporter similar to bacterial xylose permeases. We found that the degree of homology for xylose is not higher than the homology for other known sugar/proton symporters and that other members of the major facilitator superfamily, such as myo-inositol transporter INT2 (35) and polyol transporter PLT6 (36), show an even higher degree of homology to these bacterial xylose transporters. However, we could not detect any transport activity for xylose in vacuoles from *AtVGT1*-expressing yeasts. Because of the described subcellular localization and transport properties, we named the protein AtVGT1.

The observed ATP-dependency for glucose import across the tonoplast strongly suggests an active transport step, which would allow accumulation of glucose into vacuoles *in planta*. Several studies of the subcellular sugar distribution in a variety of plant species have documented significantly higher hexose concentrations in the vacuoles in comparison to the cytosol (refs. 24, 25, and 37 and G. Lohaus, personal communication). Heineke *et al.* (25) measured up to 98% of the hexoses in the vacuoles of tobacco wild-type leaves and concluded that leaf vacuoles contain transporters for the active uptake of glucose and fructose against a high concentration gradient. Plant vacuoles contain a proton-translocating ATPase that generates an inside acidic pH and a positive membrane potential (38), and it was shown that glucose uptake was accompanied by a proton efflux in a 1:1 stoichiometry that clearly supports the model of a glucose/H^+ antiport (16). The described features of AtVGT1 very well fit into this model.

First-expression analyses using RT-PCR detected high expression levels of *AtVGT1* in flowers, basal *AtVGT1* expression in leaves and stems, and no expression in roots. To analyze *AtVGT1* expression in more detail, we generated *AtVGT1*-promoter/*GUS* plants. However, in these reporter plants, *GUS* expression was only detectable in pollen. We then compared our results to expression data from microarray experiments available in the Genevestigator database. Here we found that, in addition to the high transcript levels in pollen (39), *AtVGT1* is expressed at low basal levels in various tissues and organs. One possible reason for the differences in GUS reporter expression and expression data found by RT-PCR and microarray analyses could be an intragenic expression control. Although relatively unusual in plants, a number of studies have shown that gene expression can also be controlled by regulatory elements outside the 5′ region (40), and recently it was shown that the expression of some sugar transporter genes also is regulated by intragenic sequences (41). Furthermore, according to the Genevestigator database, basal *AtVGT1* expression remains unaltered under most tested conditions (endogenous and exogenous factors). Although *AtVGT1* expression is increased ≈2-fold in response to nematode infection (42), the very low expression level in roots even after induction speaks against an important role of *AtVGT1* in nematode defense.

Finally, to determine the physiological function of *AtVGT1* in vivo, we analyzed two independent *Atvgt1* mutant lines and found impairment of important developmental processes. Most strikingly, in both mutant lines flowering was delayed by 9–14 days compared with wild-type lines. In addition, ≈20% of the *Atvgt1*-knockout seeds failed to germinate. According to the Genevestigator database, *AtVGT1* displays slightly elevated expression levels in seeds and in the shoot apex above the otherwise basal levels. Both effects, reduced seed germination as well as late flowering with retarded growth of the shoot, support the existence of a possible function of vacuolar hexose accumulation in the formation or maintenance of cell turgor to drive cell expansion. Further support for such a role of vacuolar hexoses comes from the functional analysis of vacuolar invertase knockouts that are defective in root elongation (43) and from the finding that hexose accumulation accounts for a large proportion of the osmotic potential in the cell elongation zone of maize root tips (44).

The impairment of seed germination and flowering observed in the *Atvgt1* mutant lines is only partial, indicating that the plant can somehow overcome this loss of AtVGT1 transport function.

Because *AtVGT1* is a member of a small gene family, it is possible that another homolog like At5g17010 can replace *AtVGT1* function. Interestingly, the At5g17010 gene product also was shown to be localized in the tonoplast (unpublished data). However, it also is possible that other more indirect effects, like the up-regulation of transporters for other osmolytes, can compensate for the absence of a functional AtVGT1 transporter.

We have identified a family of sugar transporters in *Arabidopsis*. One member, AtVGT1, was shown to be localized in the tonoplast. Most importantly, using yeast as a heterologous expression system, we were able to demonstrate transport activity for this previously unknown vacuolar sugar transporter. The implied potential to manipulate sugar fluxes in crop plants by changing the expression and/or activity of these vacuolar transporters is of great agricultural importance.

Materials and Methods

Strains and Growth Conditions. *Escherichia coli* strain DH5α (45) was used for cloning. Heterologous expression was performed in *S. cerevisiae* strain EBY.VW4000 (provided by E. Boles, University of Düsseldorf, Düsseldorf, Germany) (46). Yeast transformation was as described (47). *Ar. thaliana* Col-0 was grown in a greenhouse in potting soil or on agar medium in growth chambers under a 16-h light/8-h dark regime at 22°C and 55% relative humidity. Transformations of *Ar. thaliana* were performed with *Agrobacterium tumefaciens* strains GV3101 (48).

Isolation of a Full-Length cDNA Clone of *AtVGT1*. A 1,522-bp PCR fragment containing the complete *AtVGT1* coding sequence was amplified from flower-specific cDNA by using primers AtXYL1c −15f (CAA GCT TCA ATT GCC ATG GGG TTT GAT) and AtXYL1c +1522r (GAG TCA ATT GTT AGA GAC ATT TGG CTT CAA TTT C), cloned into pGEM-T easy (pSA109), and sequenced.

Functional Characterization of *AtVGT1* by Heterologous Expression in Yeast. The *AtVGT1* cDNA fragment from pSA109 was ligated into the unique EcoRI site of the *S. cerevisiae/E. coli* shuttle vector NEV-E (49), in both sense and antisense orientation, yielding constructs pSA114s and pSA114as, respectively. Both constructs were then used to transform the hexose transporter-deficient *S. cerevisiae* strain EBY.VW4000 (46), yielding strains SAY114s and SAY114as. Transport tests were performed with isolated vacuoles from transgenic yeasts. To isolate yeast vacuoles, a modified protocol of Ohsumi and Anraku (32) was used. In brief, yeast cells were grown to OD_{600} of 0.5–1. Cells were harvested at 4,500 × *g* for 5 min, washed twice with distilled water, and resuspended in 30 ml of spheroplasting buffer [1 M sorbitol containing 80 units of zymolyase dissolved in 500 μl of 50 mM Tris·HCl (pH 7.5), 1 mM EDTA, 50% glycerol]. After incubation at 29°C for 1 h, spheroplasts were harvested by centrifugation (2,200 × *g* for 5 min), washed twice with 1 M sorbitol and resuspended in buffer A (10 mM Mes-Tris, pH 6.9/0.1 mM $MgCl_2$/12% Ficoll). Spheroplast lysis was further improved by using a dounce homogenizer. Cell debris was removed by centrifuging the homogenate (2,200 × *g* for 10 min). The supernatant (10 ml) was overlayered with fresh buffer A (20 ml) and centrifuged for 1 h at 60,000 × *g* (swing-out rotor). Floating vacuoles were harvested from the surface and resuspended in 2× buffer C (20 mM Mes-Tris, pH 7.9/5 mM $MgCl_2$/25 mM KCl). For transport assays with isolated yeast vacuoles, the standard reaction (100 μl) consisted of 50 μg of vacuolar protein, 20 mM Mes-Tris (pH 7.9), 4 mM $MgCl_2$, 4 mM ATP, 1 mM cold substrate, and 0.1 μCi of ^{14}C-labeled substrate. This reaction mixture was incubated at 29°C for 5 min without substrate. The transport assay process was started by adding the substrate and stopped by diluting the mixture with 2 ml of ice-cold 2× buffer C. Vacuoles were quickly recovered on a nitrocellulose filter (0.2 μm pore size) and washed with 2 ml of cold 2× buffer C. The radioactivity was measured in a scintillation counter by adding the nitrocellulose filter to 4 ml of scintillation mixture.

***AtVGT1* Expression Analysis Using GUS Reporter Plants and RT-PCR.** A 1,939-bp promoter fragment from *Arabidopsis* genomic DNA was amplified by PCR with primers AtXYL1g −1876f(SphI) (GAT GTT GGA AGC ATG CAT ATA TGG) and AtXYL1g +66r (CGA TAA TGA GAA AAG CGA AAC C) and then digested with SphI and NcoI restriction enzymes. The resulting 1,816-bp SphI/NcoI fragment was ligated into the vector pAF6, which is a pUC19-based plasmid that harbors the *GUS* reporter gene (36), and sequenced, yielding construct pSA103. A 3.15-kb XmaI/EcoRI fragment comprising the *AtVGT1* promoter followed by the *GUS* gene and the *Nos* terminator was cloned into the plant vector pGPTV-BAR (50), yielding pSA104. *Arabidopsis* plants were transformed by floral dip using *Ag. tumefaciens* strain GV3101 (48), which harbors the construct pSA104 (51). Transformation of *Arabidopsis* resulted in 13 independent Basta-resistant transformants, and reporter gene activity was studied in all of these plants in the T1 generation. RT-PCRs were performed by using total RNA from different tissues and *AtVGT1*-specific primers AtXYL1g +2326f (GGG ACA AGG AAA TGG GGA GAA TC) and AtXYL1g +3052r (CGC TAA CAC CAC AAA GAA GTA A) or Actin2-specific primers AtACT2g +846f (ATT CAG ATG CCC AGA AGT CTT GTT) and AtACT2g +1295r (GAAACATTTTCTGTGAACGATTCCT), yielding 407- and 362-bp products, respectively.

Transient Expression of AtVGT1-*GFP* in *Arabidopsis* Protoplasts. For transient expression of *AtVGT1–GFP* fusions, the *AtVGT1* coding sequence was PCR-amplified with the AtXYL1c −20f (CAT ACC AAG CTT CCG TAG CC) and AtXYL1c +1526r (AGA TGA GTA ACC ATG GAG AGA CAT TTG) and inserted into the unique NcoI-cloning site of pSO35e (a pUC19-based plasmid that harbors the *GFP* reporter gene). With the resulting plasmid pSA119, *Arabidopsis* protoplasts were transformed by polyethylene glycol transformation modified according to the methods of Abel and Theologis (52), and *AtVGT1-GFP* expression was monitored by confocal microscopy.

***Arabidopsis* Mutant Lines Carrying a T-DNA Insertion in the *AtVGT1* Gene.** For *Arabidopsis* T-DNA insertion lines, the insertion site was reconfirmed and lines with a homozygous T-DNA insertion were identified. For SALK_000988 insertion lines, the T-DNA insertion was verified by genomic PCR with the T-DNA-specific primer LBa1 (CGA TGG CCC ACT ACG TGA ACC AT) and AtXYL1g +408r (CCT TTT CAG CAG TAA TCC CAC C). The insertion was localized in the 5′ UTR at position −1 (relative to the start-ATG) by sequencing the 428-bp PCR product. Lines with homozygous T-DNA insertion were identified by genomic PCR with the *AtVGT1*-specific primers AtXYL1g −1382f (CAT TGA AAC AAG CAA TCA CTT TG) and AtXYL1g +408r. The same procedure was used for line SAIL_669_D03, in which the insertion was localized at position +2760 by using primers LB3 (TAG CAT CTG AAT TTC ATA ACC AAT CTC GAT ACA C) and AtXYL1g +3052r (CGC TAA CAC CAC AAA GAA GTA A). Homozygous T-DNA insertion lines were identified by RT-PCR with total RNA from flowers and *AtVGT1*-specific primers AtXYL1g +2326f and AtXYL1g +3052r.

We thank Rebecca Günther and Gudrun Steingräber for excellent technical help, Stefan Hoth for assistance in confocal microscopy, and Sabine Strahl and Norbert Sauer for critically reading the manuscript. This work was supported by Deutsche Forschungsgemeinschaft Grant Bu 973/5 (to M.B.).

1. Lemoine R (2000) *Biochim Biophys Acta* 1465:246–262.
2. Lalonde S, Wipf D, Frommer WB (2004) *Annu Rev Plant Biol* 55:341–372.
3. Williams LE, Lemoine R, Sauer N (2000) *Trends Plants Sci* 5:283–290.
4. van Bel AJE (2003) *Plant Cell Environ* 26:125–149.
5. Truernit E (2001) *Curr Biol* 11:R169–R171.
6. Sherson SM, Alford HL, Forbes SM, Wallace G, Smith SM (2003) *J Exp Bot* 54:525–531.
7. Weise SE, Schrader SM, Kleinbeck KR, Sharkey TD (2006) *Plant Physiol* 141:879–886.
8. Getz HP, Klein M (1995) *Plant Physiol* 107:459–467.
9. Briskin DP, Thornley WR, Wyse RE (1985) *Plant Physiol* 78:871–875.
10. Getz HP (1991) *Planta* 185:261–268.
11. Doll S, Rodier F, Willenbrink J (1979) *Planta* 144:407–411.
12. Thom M, Komor E, Maretzki A (1982) *Plant Physiol* 69:1320–1325.
13. Keller F (1992) *Plant Physiol* 98:442–445.
14. Rausch T (1991) *Physiol Plant* 82:134–142.
15. Martinoia E, Massonneau A, Frangne N (2000) *Plant Cell Physiol* 41:1175–1186.
16. Thom M, Komor E (1984) *FEBS Lett* 173:1–4.
17. Martinoia E, Kaiser G, Schramm MJ, Heber U (1987) *J Plant Physiol* 131:467–478.
18. Buttner M, Sauer N (2000) *Biochim Biophys Acta* 1465:263–274.
19. Sauer N, Baier K, Gahrtz M, Stadler R, Stolz J, Truernit E (1994) *Plant Mol Biol* 26:1671–1679.
20. Chiou TJ, Bush DR (1996) *Plant Physiol* 110:511–520.
21. Endler A, Meyer S, Schelbert S, Schneider T, Weschke W, Peters SW, Keller F, Baginsky S, Martinoia E, Schmidt UG (2006) *Plant Physiol* 141:196–207.
22. Weschke W, Panitz R, Sauer N, Wang Q, Neubohn B, Weber H, Wobus U (2000) *Plant J* 21:455–467.
23. Weise A, Barker L, Kuhn C, Lalonde S, Buschmann H, Frommer WB, Ward JM (2000) *Plant Cell* 12:1345–1355.
24. Voitsekhovskaja OV, Koroleva OA, Batashev DR, Knop C, Tomos AD, Gamalei YV, Heldt HW, Lohaus G (2006) *Plant Physiol* 140:383–395.
25. Heineke D, Wildenberger K, Sonnewald U, Willmitzer L, Heldt HW (1994) *Planta* 194:29–33.
26. Wagner GJ (1979) *Plant Physiol* 64:88–93.
27. Pollock CJ, Farrar J, Koroleva OA, Gallagher JA, Tomos AD (2000) *Rev Bras Bot* 23:349–357.
28. Marger MD, Saier MH, Jr (1993) *Trends Biochem Sci* 18:13–20.
29. Reifenberger E, Boles E, Ciriacy M (1997) *Eur J Biochem* 245:324–333.
30. Scholz-Starke J, Buttner M, Sauer N (2003) *Plant Physiol* 131:70–77.
31. Schneidereit A, Scholz-Starke J, Buttner M (2003) *Plant Physiol* 133:182–190.
32. Ohsumi Y, Anraku Y (1981) *J Biol Chem* 256:2079–2082.
33. Zimmermann P, Hirsch-Hoffmann M, Hennig L, Gruissem W (2004) *Plant Physiol* 136:2621–2632.
34. Deutsch M, Long M (1999) *Nucleic Acids Res* 27:3219–3228.
35. Schneider S, Schneidereit A, Konrad KR, Hajirezaei MR, Gramann M, Hedrich R, Sauer N (2006) *Plant Physiol* 141:565–577.
36. Klepek YS, Geiger D, Stadler R, Klebl F, Landouar-Arsivaud L, Lemoine R, Hedrich R, Sauer N (2005) *Plant Cell* 17:204–218.
37. Moore B, Palmquist DE, Seemann JR (1997) *Plant Physiol* 115:241–248.
38. Thom M, Komor E (1984) *Eur J Biochem* 138:93–99.
39. Pina C, Pinto F, Feijo JA, Becker JD (2005) *Plant Physiol* 138:744–756.
40. Taylor CB (1997) *Plant Cell* 9:273–275.
41. Sivitz AB, Reinders A, Johnson ME, Krentz AD, Grof CP, Perroux JM, Ward JM (2006) *Plant Physiol* 143:188–198.
42. Hammes UZ, Schachtman DP, Berg RH, Nielsen E, Koch W, McIntyre LM, Taylor CG (2005) *Mol Plant–Microbe Interact* 18:1247–1257.
43. Sergeeva LI, Keurentjes JJ, Bentsink L, Vonk J, van der Plas LH, Koornneef M, Vreugdenhil D (2006) *Proc Natl Acad Sci USA* 103:2994–2999.
44. Sharp RE, Hsiao TC, Silk WK (1990) *Plant Physiol* 93:1337–1346.
45. Hanahan D (1983) *J Mol Biol* 166:557–580.
46. Wieczorke R, Krampe S, Weierstall T, Freidel K, Hollenberg CP, Boles E (1999) *FEBS Lett* 464:123–128.
47. Gietz D, St Jean A, Woods RA, Schiestl RH (1992) *Nucleic Acids Res* 20:1425.
48. Holsters M, Silva B, Van Vliet F, Genetello C, De Block M, Dhaese P, Depicker A, Inze D, Engler G, Villarroel R, *et al.* (1980) *Plasmid* 3:212–230.
49. Sauer N, Stolz J (1994) *Plant J* 6:67–77.
50. Becker D, Kemper E, Schell J, Masterson R (1992) *Plant Mol Biol* 20:1195–1197.
51. Clough SJ, Bent AF (1998) *Plant J* 16:735–743.
52. Abel S, Theologis A (1994) *Plant J* 5:421–427.
53. Bowman JL (1993) *Arabidopsis: An Atlas of Morphology and Development* (Springer, Berlin).